Mathematical Biosciences and Engineering

http://www.aimspress.com/journal/MBE

MBE, 18(6): 8857–8882.
DOI: 10.3934/mbe.2021437
Received: 10 June 2021
Accepted: 07 October 2021
Published: 15 October 2021

Research article

Dynamical analysis of an aquatic amensalism model with non-selective harvesting and Allee effect

Huanyi Liu[1,2], Hengguo Yu[1,2,*], Chuanjun Dai[1,3], Zengling Ma[1,3], Qi Wang[1,3] and Min Zhao[1,3,*]

[1] Key Laboratory for Subtropical Oceans & Lakes Environment and Biological Resources Utilization Technology of Zhejiang, Wenzhou University, Wenzhou, Zhejiang, 325035, China
[2] School of Mathematics and Physics, Wenzhou University, Wenzhou, Zhejiang, 325035, China
[3] School of Life and Environmental Science, Wenzhou University, Wenzhou, Zhejiang, 325035, China

* **Correspondence:** Email: yuhengguo5340@163.com, zhaomin-zmcn@tom.com.

Abstract: In this paper, in order to explore the inhibition mechanism of algicidal bacteria on algae, we constructed an aquatic amensalism model with non-selective harvesting and Allee effect. Mathematical works mainly gave some critical conditions to guarantee the existence and stability of equilibrium points, and derived some threshold conditions for saddle-node bifurcation and transcritical bifurcation. Numerical simulation works mainly revealed that non-selective harvesting played an important role in amensalism dynamic relationship. Meanwhile, we proposed some biological explanations for transcritical bifurcation and saddle-node bifurcation from the aspect of algicidal bacteria controlling algae. Finally, all these results were expected to be useful in studying dynamical behaviors of aquatic amensalism ecosystems and biological algae controlling technology.

Keywords: amensalism model; Allee effect; harvest; transcritical bifurcation; saddle-node bifurcation

1. Introduction

Algae and some algicidal bacteria can constitute a unique micro-ecological environment system, and their interaction is similar to symbiosis [1]. However, some algicidal bacteria can release specific or non-specific extracellular substances to inhibit algae or kill algal cells, especially which can produce antibiotics to inhibit the growth of algae population. Thus, the relationship between algae and algicidal bacteria is similar to amensalism. Dakhama et al. [2] pointed out that Pseudomonas aeruginosa could produce a lot of antibiotics to inhibit the growth of other bacteria and algae. Kawano et al. [3] confirmed that bacterial strain pk654 could produce antibiotic thiotropocin to inhibit Skeletonema medialis and Heterosigma. Xiao et al. [4] concluded that the extracellular metabolites of actinomycete AN02 had

a good inhibitory effect on Microcystis aeruginosa. Choi et al. [5] pointed out that the growth of Microcystis could be well inhibited by Streptomyces neogawaensis. Thus, it is obvious that because harmful algal blooms have become one of the most urgent ecological and environmental problems in the world, the algal-bacterial interaction will pose the possible of using some algicidal bacteria for biological control of algal blooms [6]. Although a large number of literatures have studied dynamic relationship between algae and bacteria, and some excellent research results have also been given, it is a pity that the lysing dynamic process and characteristics of algicidal bacteria are still unclear. Therefore, it is necessary to find a new way to better understand the dynamic mechanism between algae and algicidal bacteria. However, as far as we are concerned, it is possible to seek a relatively new way to reveal the dynamic inhibition mechanism of algicidal bacteria on algae by using mathematical models and dynamic analysis technology.

In natural ecosystems, the amensalism relationship is one of the symbiotic relationships between two kinds of organisms [7]. When two kinds of organisms live together, one of them does not get benefits, the other species is negatively by the presence of the first species, but it doesn't have to die. Even if a individual experiences death, the negatively-impacted species will not die. At the same time, in the amensalism relationship, one organism can inhibit and harm another organism, even kill each other, but it does not directly benefit or harm itself. For example, plants in the walnut family can secrete juglone to inhibit the growth of other plants nearby, and penicillin produced by Penicillium can inhibit Gram-positive bacteria [8].

In recent ten years, the research on amensalism relationship and population dynamic model has achieved many excellent results. Sun [9] firstly proposed the following population amensalism model:

$$\begin{cases} \frac{dx}{dt} = r_1 x(\frac{k_1 - x - Ty}{k_1}), \\ \frac{dy}{dt} = r_2 y(\frac{k_2 - y}{k_2}), \end{cases} \tag{1.1}$$

where r_1 and r_2 are respectively the intrinsic growth rate of two species, k_1 and k_2 are respectively the environmental carrying capacity of two species, T represents the coefficient of effect single y on x. The author investigated the stability of all equilibrium points of this model (1.1). Based on the model (1.1), two population amensalism Lotka-Volterra model were proposed to investigate the permanence and extinction [10, 11], and discuss the stability using the characteristic theory [12]. Wu [13] constructed a two species amensalism model with non-monotonic functional response argued by using the linear functional response to depict the influence of the second species to the first species, which can be depicted as follows:

$$\begin{cases} \frac{dx_1}{dt} = x_1(a_1 - b_1 x_1 - \frac{cx_2}{d + x_2^2}), \\ \frac{dx_2}{dt} = x_2(a_2 - b_2 x_2), \end{cases} \tag{1.2}$$

where a_1, a_2, b_1, b_2, c, d are all positive constants. He studied the global dynamics of all the possible equilibrium points of the model (1.2). Guan and Chen [14] proposed a two species amensalism model with Beddington-DeAngelis functional response and Allee effect on the second species, which can be described as follows:

$$\begin{cases} \frac{dx}{dt} = x(a_1 - b_1 x - \frac{cy}{1 + mx + ny}), \\ \frac{dy}{dt} = y(a_2 - b_2 y)\frac{y}{u + y}, \end{cases} \tag{1.3}$$

where $\frac{y}{u+y}$ represents the Allee effect, and u is a positive constant, which can describe the intense of the Allee effect. They discussed the global dynamics of all the possible equilibrium points of the model

(1.3), and found that the Allee effect had no influence on the final density of the species, but could cause the trajectories of the model (1.3) approaching the equilibrium solution more slowly. Drawing lessons from the model (1.2) and (1.3), a large number of amensalism ecological models have been constructed and studied, such as: a three-species model with partial harm relations [15], a Holling type commensal symbiosis model involving Allee effect [16], a non-selective harvesting Lotka-Volterra amensalism discrete model [17], a non-autonomous Lotka-Volterra amensalism model [18], and an amensalism model with weak Allee effect [19]. However, as far as we know, there is little research on aquatic amensalism model based on the inhibition mechanism of algicidal bacteria on algae.

Courchamp et al. [20] pointed out that the survival and reproduction of algicidal bacteria had a certain Allee effect, hence, the Allee effect must be taken into account in the process of establishing an aquatic amensalism model. Allee effect was first proposed by ecologist Allee in 1931 [21], since then, Stephens and other researchers summarized the previous research results and gave a clear definition of Allee effect. This definition was the positive correlation between the number or population density of the same species and any aspect of individual fitness [22–24]. Furthermore, such relationship was also known as inverse density dependence [23, 24], depensation [25] and positive density dependence [26, 27]. At the same time, as more and more scholars have paid attention to Allee effect in some mathematical biological models, and given a large number of excellent research results in the papers [28–32]. Rebelo and Soresina [28] gave some general conditions for coexistence of prey and predator in the case of weak and strong Allee effect. Kumar et al. [29] concluded that Allee effect could generate or destroy the interior attractor. Sen et al. [30] pointed out that increasing value of Allee parameter could turn the system more structurally stable. Bai et al. [31] pointed out that strong Allee effect in the basal prey could increase the extinction risk of not only the basal prey but also the intraguild prey. Tripathi et al. [32] found that the introduction of Allee effect could induce more rich dynamics and compel the system to be more sensitive to initial population densities. Obviously, Allee effect has some serious effects on the dynamic characteristics of ecological population. In addition, with more and more examples of Allee effect in the ecological nature, ecologists and biological mathematicians will pay more and more attention to the research of Allee effect, and it is possible that more and more excellent research results will be published in the near future.

During the experiment of algicidal bacteria inhibiting growth dynamics of algae population, in order to ensure the sustainability of this experiment, it is necessary to consider an ecological harvest in this aquatic amensalism model, which is a favorable economic tool to realize the high unity and sustainable development of economic take-off and environmental protection [33]. In ecological model, harvest is one of critical factors, which can grab the attention among researchers due to its importance in resource management and sustainable development from the biological and economic standpoints [34]. Therefore, a large number of excellent research results have been given in these papers. Ang et al. [34] derived some optimal thresholds for predator harvesting to give maximum financial profit for sustaining the fishery resources. Clark [35] systematically and orderly investigated harvesting behaviors of natural populations. Clark et al. [36] proposed mathematical models of exploited fish stocks through a dynamic aggregation process. Das et al. [37] investigated a prey-predator fishery model to explore the optimal harvesting policy. Das et al. [38] solved the problem of determining the optimal harvesting policy of a predator-prey model. Liu and Huang [39] inquired into a series of harvesting problems of a harvested predator-prey model. Bellier et al. [40] demonstrated that two different harvesting strategies were needed to optimize the annual yield of predators and prey. Datta et al. [41] found that the age-selective

harvesting system could undergo a Hopf bifurcation. Li et al. [42] discussed stability and bifurcations of a bio-economic differential algebraic predator-prey model. Gupta et al. [43] investigated numerous kinds of bifurcations of a predator-prey model with nonlinear predator harvesting. Guin et al. [44] studied the effect of harvesting on the control of spatial pattern formation. Guin et al. [45] pointed out that harvesting effort could play a vital function for geological conservation. Guin and Acharya [46] proposed that the effect of harvesting could play a significant role on the control of spatial pattern formation. Thus, it can be seen from the above that harvesting behavior has an important impact on population dynamics. Moreover, with the circular development of ecological economics, we believe that more and more attention has been paid to ecological harvest in the implementation of ecological algae control strategy.

At present, it is useful to carry out ecological model to study the algae control behavior of algicidal bacteria. This is because that ecological model can form three basic of studying biological system, namely: trophic level analysis, system perspective and dynamic view [47, 48], which can improve the understanding of the interactions between populations and their dependence on internal and external conditions [49, 50]. Therefore, in recent decades, the research of ecological model has developed rapidly, and some excellent models have been obtained in the paper. Balram et al [51] proposed a two-dimensional prey-predator system, and found that the negative feedback delay and gestation delay could destabilize the behavior of the system. Guin et al. [52–54] investigated dynamics of predator-prey system, and achieved a series of important and meaningful results(Turing instability can be affected by nonlinear harvesting [52], prey harvesting has a significant effect on the spatiotemporal pattern formations of predator-prey systems [53], and prey harvesting can induce diffusion-driven instability resulting in stationary Turing patterns [54]). Wang and Yu [55] obtained some sufficient and threshold conditions to guarantee the occurrence of saddle-node, pitchfork, and Hopf bifurcations. Li et al. [56] constructed a new aquatic ecological model to describe the aggregation effect of Microcystis aeruginosa, and investigated some critical threshold conditions through the discovery of transcritical bifurcation, saddle-node bifurcation, Hopf bifurcation and Bogdanov-Takens bifurcation. Han et al. [57,58] investigated how fear effect and refuge to pattern formation in predator=prey model. However, facing more and more natural ecological environment problems, the research on ecological model and its related applications still needs to be strengthened and deepened. Based on the above overview, the main aim of the paper is to explore the inhibition mechanism of algicidal bacteria on algae by means of bifurcation dynamic behaviors of a new aquatic amensalism model. On this basis, we clarify biological meaning of transcritical bifurcation and saddle-node bifurcation from the aspect of algicidal bacteria controlling algae.

2. Construction of ecological model

In order to describe the dynamic relationship between algae and algicidal bacteria (it can produce antibiotic) by using ecological mathematical modeling, some modeling assumptions are given as follows:

(1) The growth space of algicidal bacteria and algae is semi closed water environment, species concentration is always evenly distributed in space and changed instantaneously with time t, $x(t)$ and $y(t)$ represent respectively the density of algae and algicidal bacteria. Furthermore, we demand that algicidal bacteria can produce antibiotic to inhibit algal growth.

(2) The paper [59] pointed out that the growth curve of algicidal bacteria (Microbacterium oleivoran) is in line with logistic model, and then the survival and reproduction of algicidal bacteria have Allee effect [20]. Thus, we assume that the dynamic growth function of algicidal bacteria y is $y(a_2 - b_2y)F(y)$ with intrinsic growth rate a_2 and maximum environmental capacity $\frac{a_2}{b_2}$ as well as the Allee effect $F(y) = \frac{y}{u+y}$, where u is Allee effect constant, the larger the value of u is, the stronger the Allee effect is. At the same time, we also suppose that the dynamic growth function of algae x is $x(a_1 - b_1x)$ with intrinsic growth rate a_1 and maximum environmental capacity $\frac{a_1}{b_1}$, this is because that a large number of experiments have proved that logistic growth function is most consistent with the growth trend of algae in nature [60].

(3) In order to prevent algal blooms from breaking out or rotting later, the algae needs to be salvaged or harvested regularly. At the same time, because algicidal bacteria are attached to algae, the salvage or harvest of the algae will lead to the salvage or harvest of some algicidal bacteria. Hence, we presume that the harvesting functions of algae and algicidal bacteria are q_1mEx and q_2mEy respectively, where q_i is the catchability co-efficient of the ith species, E is the combined capture effort used to harvest, and $m(0 < m < 1)$ is the fraction of the stock available for harvesting.

(4) As everyone knows, the survival and reproduction of algicidal bacteria are dependent on a certain number of algae. Meanwhile, if the density of algicidal bacteria is relatively small, it needs to attract nutrients for rapid propagation. Thus algicidal bacteria can form a competitive relationship with algae, and also secrete a large number of antibiotics to inhibit the growth of algae. However, with the increase of algicidal bacteria density, the living space of algicidal bacteria will gradually reduce, and algicidal bacteria will form internal competition, which leads to the need for a large number of algae, and then the inhibition effect of algal growth will be weakened. In other words, the inhibition of algicidal bacteria on algae is a humped function and declines with the high densities of algicidal bacteria and internal competitive relationship. Thus, we give an inhibition function of algicidal bacteria on algal growth $\frac{cxy}{d+y^2}$ with the half saturation constant d and the maximum value of the per capita reduction rate c.

Based on the above hypothesis and the inspiration of some works [9, 13, 14], we will propose an aquatic amensalism model with non-selective harvesting and Allee effect, which can be described by the following differential equation:

$$\begin{cases} \frac{dx}{dt} = x(a_1 - b_1x) - \frac{cxy}{d+y^2} - q_1mEx, \\ \frac{dy}{dt} = y(a_2 - b_2y)\frac{y}{u+y} - q_2mEy. \end{cases} \tag{2.1}$$

In this paper, we firstly give some sufficient conditions to guarantee the existence and stability of all possible equilibrium points of the model (2.1), which contain the survival mode of algae and algicidal bacteria, and analyze some critical conditions to ensure that the model (2.1) can occur saddle-node bifurcation and transcritical bifurcation, which mainly reflect the dynamic process of the survival and evolution of algae and algicidal bacteria. Secondly, the relevant dynamic simulation experiments of the model (2.1) are implemented to verify the feasibility of the theoretical results and reveal some specific dynamic behaviors, which can visually explain the interaction trend and dynamic evolution trend of algae and algicidal bacteria. Finally, based on the results of numerical simulation, we explore how Allee effect and harvest affect the intrinsic dynamics of the model (2.1), and analyze the biological significance of some particular bifurcation dynamics(saddle-node bifurcation and transcritical bifurcation.

3. Results of mathematical analysis

3.1. Equilibrium points and their stability

In this section, the existence and stability of all possible equilibrium points of the model (2.1) will be discussed carefully, this is because that equilibrium point is a special solution of the model (2.1), which has special ecosystem significance. In order to obtain all possible equilibrium points of the model (2.1), we consider the following equation:

$$\begin{cases} x(a_1 - b_1 x) - \frac{cxy}{d+y^2} - q_1 mEx = 0, \\ y(a_2 - b_2 y)\frac{y}{u+y} - q_2 mEy = 0. \end{cases} \tag{3.1}$$

All possible equilibrium points are now the points of intersection of these equations, thus it is easy to obtain that the model (2.1) has a trivial equilibrium point $E_0(0, 0)$ and algicidal bacteria extinction equilibrium point $E_1(\frac{a_1 - q_1 mE}{b_1}, 0)$ with $a_1 - q_1 mE > 0$. For other boundary and positive equilibrium of the model (2.1), we need consider the positive solutions of the following equations:

$$\begin{cases} x = \frac{1}{b_1}(a_1 - q_1 mE - \frac{cy}{d+y^2}), \\ b_2 y^2 - (a_2 - q_2 mE)y + q_2 mEu = 0. \end{cases} \tag{3.2}$$

We suppose that Δ is denoted the discriminant of the second equation of (3.2) and express Δ in terms of m, i.e., $\Delta(m) = q_2^2 E^2 m^2 - (2a_2 + 4b_2 u)q_2 mE + a_2^2$, as well as m_1 and m_2 is some roots of $\Delta(m)$. Thus, we can easily calculate that

$$m_1 = \frac{a_2 + 2b_2 u - 2\sqrt{b_2 u(a_2 + b_2 u)}}{q_2 E}, m_2 = \frac{a_2 + 2b_2 u + 2\sqrt{b_2 u(a_2 + b_2 u)}}{q_2 E}.$$

Since all the parameters are positive, then $m_2 > m_1 > 0$. Thus, we can acquire the following theorem.

Theorem 1. For algae population free equilibrium points:

(1) If $m > m_1$, then the model (2.1) has no algae population free equilibrium point.

(2) If $0 < m < m_1$, then the model (2.1) has two algae population free equilibrium points $E_2(0, y_1^*)$ and $E_3(0, y_2^*)$, where $y_{1,2}^* = \frac{a_2 - q_2 mE \pm \sqrt{(a_2 - q_2 mE)^2 - 4b_2 q_2 mEu}}{2b_2}$.

(3) If $m = m_1$, then the model (2.1) has a unique algae population free equilibrium point $E_4(0, y_3^*)$, where $y_3^* = \frac{a_2 - q_2 mE}{2b_2}$.

Our method of proving this theorem is similar to Hu and Cao [61] (see Theorem 1). For the sake of brevity, here we omit it.

Theorem 2. For all interior equilibrium points, we have:

(1) If $m > m_1$ or $m = m_1$, $q_1 \geq g(y_3^*)$ or $0 < m < m_1$, $q_1 \geq \max\{g(y_1^*), g(y_2^*)\}$, then the model (2.1) has no interior equilibrium point, where
$g(y_1^*) = \frac{a_1}{mE} - \frac{cy_1^*}{mE(d+y_1^{*2})}$, $g(y_2^*) = \frac{a_1}{mE} - \frac{cy_2^*}{mE(d+y_2^{*2})}$, $g(y_3^*) = \frac{a_1}{mE} - \frac{cy_3^*}{mE(d+y_3^{*2})}$.

(2) If $m = m_1$ and $q_1 < g(y_3^*)$, then the model (2.1) has a unique interior equilibrium point $E_3^*(x_3^*, y_3^*)$, where $x_3^* = \frac{1}{b_1}(a_1 - q_1 mE - \frac{cy_3^*}{d+y_3^{*2}})$, $y_3^* = \frac{a_2 - q_2 m_1 E}{2b_2}$.

(3) If $0 < m < m_1$, then:

(a) If $q_1 < \min\{g(y_1^*), g(y_2^*)\}$, then the model (2.1) has two distinct interior equilibrium points $E_1^*(x_1^*, y_1^*)$ and $E_2^*(x_2^*, y_2^*)$, where $x_{1,2}^* = \frac{1}{b_1}(a_1 - q_1 mE - \frac{cy_{1,2}^*}{d+y_{1,2}^{*2}})$, $y_{1,2}^* = \frac{a_2 - q_2 mE \pm \sqrt{(a_2 - q_2 mE)^2 - 4b_2 q_2 mEu}}{2b_2}$.

(b) If $g(y_1^*) > g(y_2^*)$, $g(y_2^*) \le q_1 < g(y_1^*)$, then the model (2.1) has a unique interior equilibrium point $E_1^*(x_1^*, y_1^*)$, where x_1^* and y_1^* are the same as in case (a).

(c) If $g(y_1^*) < g(y_2^*)$, $g(y_1^*) \le q_1 < g(y_2^*)$, then the model (2.1) has a unique interior equilibrium point $E_2^*(x_2^*, y_2^*)$, where x_2^* and y_2^* are the same as in case (a).

Note that this theorem follows immediately from Theorem 1 and some straightforward computation.

Theorem 3. For all positive parameters, the model (2.1) has a boundary equilibrium point E_0, if $0 < q_1 < \frac{a_1}{mE}$, then the equilibrium point E_0 is a saddle; if $q_1 > \frac{a_1}{mE}$, then the equilibrium point E_0 is a stable node; and if $q_1 = \frac{a_1}{mE}$, then the equilibrium point E_0 is a saddle-node. Moreover, when $0 < q_1 < \frac{a_1}{mE}$, the equilibrium point E_1 exists, and it is always a stable node.

Proof: The Jacobian matrix of the model (2.1) evaluated at the equilibrium point E_0 is given by

$$J_{E_0} = \begin{pmatrix} a_1 - q_1 mE & 0 \\ 0 & -q_2 mE \end{pmatrix}.$$

Clearly, if $0 < q_1 < \frac{a_1}{mE}$, then the equilibrium point E_0 is a saddle; if $q_1 > \frac{a_1}{mE}$, then the equilibrium point E_0 is a stable node; if $q_1 = \frac{a_1}{mE}$, using the Theorem 7.1 in Chapter 2 in [62], we can obtain that the equilibrium point E_0 is a saddle-node. That is to say, two separators that can tend to the equilibrium point E_0 along the upside and underneath of the equilibrium point E_0 can separate the neighborhood of E_0 into two parts. One part is a parabolic sector, and the other part mainly consists two hyperbolic sectors. Moreover, here the parabolic sector is on the right halfplane because of $a_m > 0$.

When $0 < q_1 < \frac{a_1}{mE}$, the equilibrium point E_1 exists. The Jacobian matrix of the model (2.1) at the equilibrium point E_1 is

$$J_{E_1} = \begin{pmatrix} -(a_1 - q_1 mE) & \frac{c_1(a_1 - q_1 mE)}{b_1 d} \\ 0 & -q_2 mE \end{pmatrix}.$$

It is easy to see that the equilibrium point E_1 is always a stable node. This completes the proof.

Theorem 4.

(1) Assume that $0 < m < m_1$ holds, then the model (2.1) has two boundary equilibrium points E_2 and E_3, then we have

(a) If $q_1 < g(y_1^*)$, then the equilibrium point E_2 is a saddle; if $q_1 > g(y_1^*)$, then the equilibrium point E_2 is a stable node; if $q_1 = g(y_1^*)$, then the equilibrium point E_2 is an attracting saddle-node.

(b) If $q_1 < g(y_2^*)$, then the equilibrium point E_3 is an unstable node; if $q_1 > g(y_2^*)$, then the equilibrium point E_3 is a saddle; if $q_1 = g(y_2^*)$, then the equilibrium point E_3 is a repelling saddle-node.

(2) Assume that $m = m_1$ and $a_1 - q_1 mE - \frac{cy_3^*}{d+y_3^{*2}} \neq 0$ hold, then the model (2.1) has a boundary equilibrium point E_4, which is a saddle-node, furthermore if $q_1 < g(y_3^*)$ (or $q_1 > g(y_3^*)$), then the equilibrium point E_4 is a repelling (attracting) saddle-node.

Proof: (1) The Jacobian matrix of the model (2.1) evaluated at the equilibrium point E_2 is given by

$$J_{E_2} = \begin{pmatrix} a_1 - q_1 mE - \frac{cy_1^*}{d+y_1^{*2}} & 0 \\ 0 & \frac{-q_2 mE\sqrt{\Delta(m)}}{a_2 - b_2 y_1^*} \end{pmatrix}.$$

Apparently, if $q_1 < g(y_1^*)$, then the equilibrium point E_2 is a saddle; if $q_1 > g(y_1^*)$, then the equilibrium point E_2 is a stable node; if $q_1 = g(y_1^*)$, we again utilize Theorem 7.1 in Chapter 2 in [62] to determinate the stability of the equilibrium point E_2, which is an attracting saddle-node.

The Jacobian matrix of the model (2.1) evaluated at the equilibrium point E_3 is given by

$$J_{E_3} = \begin{pmatrix} a_1 - q_1 mE - \frac{cy_2^*}{d+y_2^{*2}} & 0 \\ 0 & \frac{q_2 mE\sqrt{\Delta(m)}}{a_2 - b_2 y_2^*} \end{pmatrix}.$$

Similarly, if $q_1 < g(y_2^*)$, the equilibrium point E_3 is an unstable node; if $q_1 > g(y_2^*)$, the equilibrium point E_3 is a saddle; if $q_1 = g(y_2^*)$, it is a repelling saddle-node.

(2) The Jacobian matrix of the model (2.1) evaluated at the equilibrium point E_4 is given by

$$J_{E_4} = \begin{pmatrix} a_1 - q_1 mE - \frac{cy_3^*}{d+y_3^{*2}} & 0 \\ 0 & 0 \end{pmatrix}.$$

It is easy to see that if $a_1 - q_1 mE - \frac{cy_3^*}{d+y_3^{*2}} \neq 0$, the equilibrium point E_4 is always a non-hyperbolic point, therefore according to the notations of Theorem 7.1 in Chapter 2 in [62], if $q_1 < g(y_3^*)$, the equilibrium point E_4 is a repelling saddle-node, and if $q_1 > g(y_3^*)$, then it is an attracting saddle-node. This completely ends the proof of Theorem 4.

Theorem 5.

(1) Assume that $0 < m < m_1$ and $q_1 < g(y_1^*)$ hold, then the positive equilibrium point E_1^* exists, which is always a stable node.

(2) Assume that $0 < m < m_1$ and $q_1 < g(y_2^*)$ hold, then the positive equilibrium point E_2^* exists, which is always a saddle.

(3) Assume that $m = m_1$ and $q_1 < g(y_3^*)$ hold, then the model (2.1) has a unique positive equilibrium point E_3^*, which is an attracting saddle-node.

We know that Theorem 5 can be proved by the same analysis as Theorem 4 above, therefore the proof of this theorem is omitted for brevity.

Based on the above discussion, we can list all the possible cases, where the stability of all possible equilibrium points of the model (2.1) may occur in Table 1 (see Appendix). Furthermore, the stability of these equilibrium points is an important theoretical basis for the later study of bifurcation dynamics.

3.2. Bifurcation analysis

In this section, we will try to discuss miscellaneous possible bifurcations of the model (2.1) and obtain some critical conditions for the occurrence of saddle-node bifurcation and transcritical bifurcation.

The saddle-node bifurcation is a best known bifurcation dynamic mechanism, which can change the model (2.1) from an unstable mode to a coexistence mode of a local stable state and a local unstable state, and also make the equilibrium point type and dynamic behavior of the model (2.1) change essentially. The transcritical bifurcation is a special bifurcation dynamic mechanism, which can make the equilibrium point of the model (2.1) exchange only through the bifurcation point, and its shape does not change, but its stability has changed essentially. Thus, the saddle-node bifurcation and the transcritical bifurcation have special biological significance in the natural evolution of ecological population, which is worthy of our in-depth exploration.

3.2.1. Saddle-node bifurcation

Here we will prove that the model (2.1) undergoes two saddle-node bifurcations, which can take place when m satisfies $m = m_{SN} = \frac{a_2+2b_2u-2\sqrt{b_2u(a_2+b_2u)}}{q_2E}$.

Theorem 6. When $m = m_{SN}$, then the model (2.1) undergoes a saddle-node bifurcation around the equilibrium point E_4 , where m is a bifurcation control parameter and $m_{SN} = m_1 = \frac{a_2+2b_2u-2\sqrt{b_2u(a_2+b_2u)}}{q_2E}$.

Proof: Based on Sotomayor's theorem [62, 63], we can prove that the model (2.1) undergoes a saddle-node bifurcation at m_{SN}. From the previous analysis, we can easily verify that $Det[J_{E_4}] = 0$ when $m_{SN} = m_1 = \frac{a_2+2b_2u-2\sqrt{b_2u(a_2+b_2u)}}{q_2E}$, which means that J_{E_4} has a zero eigenvalue $\lambda_2 = 0$. Letting $V = (v_1, v_2)^T$, $W = (w_1, w_2)^T$ be the eigenvectors of J_{E_4} and $J_{E_4^T}$ corresponding to the zero eigenvalue λ_2 respectively, then we can calculate

$$V = \begin{pmatrix} v_1 \\ v_2 \end{pmatrix} = \begin{pmatrix} 0 \\ 1 \end{pmatrix}, W = \begin{pmatrix} w_1 \\ w_2 \end{pmatrix} = \begin{pmatrix} 0 \\ 1 \end{pmatrix}.$$

Moreover, we have

$$F_m(E_4; m_{SN}) = \begin{pmatrix} -q_1Ex \\ -q_2Ey \end{pmatrix}_{(E_4;m_{SN})} = \begin{pmatrix} 0 \\ -q_2Ey_3^* \end{pmatrix},$$

$$D^2F(E_4; m_{SN})(V, V) = \begin{pmatrix} \frac{\partial^2F_1}{\partial x^2}{v_1}^2 + \frac{\partial^2F_1}{\partial xy}v_1v_2 + \frac{\partial^2F_1}{\partial y^2}{v_2}^2 \\ \frac{\partial^2F_2}{\partial x^2}{v_1}^2 + \frac{\partial^2F_2}{\partial xy}v_1v_2 + \frac{\partial^2F_2}{\partial y^2}{v_2}^2 \end{pmatrix}_{(E_4;m_{SN})} = \begin{pmatrix} 0 \\ -\frac{2b_2y_3^*}{u+y_3^*} \end{pmatrix}.$$

Using these expressions, we can get

$$W^TF_m(E_4; m_{SN}) = -q_2Ey_3^* \neq 0,$$

$$W^T[D^2F(E_4; m_{SN})(V, V)] = -\frac{2b_2y_3^*}{u+y_3^*} \neq 0.$$

Hence according to Sotomayor's theorem, we can acquire the occurrence of saddle-node bifurcation at the equilibrium point E_4 as the value of the parameter m passes through the critical threshold $m = m_{SN}$.

Analogously, when $q_1 < \min\{g(y_1^*), g(y_2^*), g(y_3^*)\}$, we know that the model (2.1) has two distinct positive equilibrium points E_1^* and E_2^* if $0 < m < m_1$, and the equilibrium point E_1^* can coincide with the equilibrium point E_2^* if $m = m_1$ and $q_1 < g(y_3^*)$, then they will vanish if $m > m_1$. Thus there is a chance

of saddle-node bifurcation around the equilibrium point E_3^* when $m = m_{SN}$. The following theorem will show the occurrence of saddle-node bifurcation around the equilibrium point E_3^* in the model (2.1).

Theorem 7. When the value of some key parameters can satisfy $m = m_{SN}$ and $q_1 < \min\{g(y_1^*), g(y_2^*), g(y_3^*)\}$, then the model (2.1) undergoes a saddle-node bifurcation around the equilibrium point E_3^*.

Proof: We assume that $q_1 < \min\{g(y_1^*), g(y_2^*), g(y_3^*)\}$ holds, and also apply Sotomayor's theorem to prove that the model (2.1) undergoes a saddle-node bifurcation at m_{SN} around the equilibrium point E_3^*. When $m_{SN} = m_1 = \frac{a_2+2b_2u-2\sqrt{b_2u(a_2+b_2u)}}{q_2E}$, it is easy to verify that $Det[J_{E_3^*}] = 0$ and $J_{E_3^*}$ has a zero eigenvalue $\lambda_2 = 0$. Letting $V = (v_1, v_2)^T$, $W = (w_1, w_2)^T$ be the eigenvectors of $J_{E_3^*}$ and $J_{E_3^{*T}}$ corresponding to the zero eigenvalue λ_2 respectively, then we can calculate

$$V = \begin{pmatrix} v_1 \\ v_2 \end{pmatrix} = \begin{pmatrix} -\frac{cx_3^*(d-y_3^{*2})}{(d+y_3^{*2})^2} \\ b_1 \end{pmatrix}, \qquad W = \begin{pmatrix} w_1 \\ w_2 \end{pmatrix} = \begin{pmatrix} 0 \\ 1 \end{pmatrix}.$$

Moreover, we have

$$F_m(E_3^*; m_{SN}) = \begin{pmatrix} -q_1Ex \\ -q_2Ey \end{pmatrix}_{(E_3^*; m_{SN})} = \begin{pmatrix} -q_1Ex_3^* \\ -q_2Ey_3^* \end{pmatrix},$$

$$\begin{aligned} D^2F(E_3^*; m_{SN})(V, V) &= \begin{pmatrix} \frac{\partial^2 F_1}{\partial x^2}{v_1}^2 + \frac{\partial^2 F_1}{\partial xy}v_1v_2 + \frac{\partial^2 F_1}{\partial y^2}{v_2}^2 \\ \frac{\partial^2 F_2}{\partial x^2}{v_1}^2 + \frac{\partial^2 F_2}{\partial xy}v_1v_2 + \frac{\partial^2 F_2}{\partial y^2}{v_2}^2 \end{pmatrix}_{(E_3^*; m_{SN})} \\ &= \begin{pmatrix} \frac{2c{b_1}^2x_3^*y_3^*(3d-y_3^{*2})}{(d+y_3^{*2})^3} \\ -\frac{2{b_1}^2b_2y_3^*}{u+y_3^*} \end{pmatrix}. \end{aligned}$$

Using these expressions, we can get

$$W^TF_m(E_3^*; m_{SN}) = -q_2Ey_3^* \neq 0,$$

$$W^T[D^2F(E_3^*; m_{SN})(V, V)] = -\frac{2{b_1}^2b_2y_3^*}{u+y_3^*} \neq 0.$$

Hence according to Sotomayor's theorem, we acquire the occurrence of saddle-node bifurcation at E_3^* when the value of critical parameter m passes through the critical threshold $m = m_{SN}$, which means that when the value of m passes from one side of $m = m_{SN}$ to the other side, the number of interior equilibrium point of the model (2.1) changes from zero to two. This completely ends the proof.

3.2.2. Transcritical bifurcation

From the above discussion, we can see that the boundary equilibrium E_0 may change its stability when the value of q_1 passes through the critical threshold $q_1 = \frac{a_1}{mE}$, and the model (2.1) may possesses another boundary equilibrium E_1. Therefore, we have the following theorem.

Theorem 8. When $q_1 = q_{1TC1}$, the model (2.1) undergoes a transcritical bifurcation around the equilibrium point E_0, where q_1 is a bifurcation control parameter and $q_{1TC1} = \frac{a_1}{mE}$.

Proof: We again use Sotomayor's theorem to prove that the model (2.1) undergoes a transcritical bifurcation at q_{1TC1} around the equilibrium point E_0. We can easily verify that $Det[J_{E_0}] = 0$, when $q_{1TC1} = \frac{a_1}{mE}$, which means that $Det[J_{E_0}]$ has a zero eigenvalue $\lambda_1 = 0$. Letting $V = (v_1, v_2)^T$, $W = (w_1, w_2)^T$ be the eigenvectors of J_{E_0} and $J_{E_0{}^T}$ corresponding to the zero eigenvalue λ_1 respectively, then we can calculate

$$V = \begin{pmatrix} v_1 \\ v_2 \end{pmatrix} = \begin{pmatrix} 1 \\ 0 \end{pmatrix}, \qquad W = \begin{pmatrix} w_1 \\ w_2 \end{pmatrix} = \begin{pmatrix} 1 \\ 0 \end{pmatrix}.$$

Moreover, we have

$$F_{q_1}(E_0; q_{1TC1}) = \begin{pmatrix} -mEx \\ 0 \end{pmatrix}_{(E_0; q_{1TC1})} = \begin{pmatrix} 0 \\ 0 \end{pmatrix},$$

$$DF_{q_1}(E_0; q_{1TC1})V = \begin{pmatrix} -mE & 0 \\ 0 & 0 \end{pmatrix}\begin{pmatrix} 1 \\ 0 \end{pmatrix}_{(E_0; q_{1TC1})} = \begin{pmatrix} -mE \\ 0 \end{pmatrix},$$

$$D^2F(E_0; q_{1TC1})(V, V) = \begin{pmatrix} \frac{\partial^2 F_1}{\partial x^2}{v_1}^2 + \frac{\partial^2 F_1}{\partial xy}v_1v_2 + \frac{\partial^2 F_1}{\partial y^2}{v_2}^2 \\ \frac{\partial^2 F_2}{\partial x^2}{v_1}^2 + \frac{\partial^2 F_2}{\partial xy}v_1v_2 + \frac{\partial^2 F_2}{\partial y^2}{v_2}^2 \end{pmatrix}_{(E_0; q_{1TC1})} = \begin{pmatrix} -2b_1 \\ 0 \end{pmatrix}.$$

Using these expressions, we can get

$$W^T F_{q_1}(E_0; q_{1TC1}) = 0,$$

$$W^T [DF_{q_1}(E_0; q_{1TC1})V] = -mE \neq 0,$$

$$W^T [D^2F(E_0; q_{1TC1})(V, V)] = -2b_1 \neq 0.$$

Thus, using Sotomayor's theorem, we acquire the occurrence of transcritical bifurcation at the equilibrium point E_0 as the value of parameter q_1 passes through the critical threshold $q_1 = q_{1TC1}$. This completely ends the proof.

Next, we discuss the existence of transcritical bifurcation at the equilibrium point E_2. Based on the previous demonstration, we can see that the number of interior equilibria will changes as the value of parameter q_1 varies. The interior equilibrium point E_1^* can bifurcate from the equilibrium point E_2 when the value of q_1 passes through the critical threshold $q_{1TC2} = g(y_1^*)$. Thus, there is a chance of transcritical bifurcation around the equilibrium point E_2 and Theorem 9 can be obtained.

Theorem 9. If $0 < m < m_1$, when the parameters satisfy the qualification $q_1 = q_{1TC2} = g(y_1^*)$, the model (2.1) undergoes a transcritical bifurcation around the equilibrium point E_2.

Proof: From the analysis of section 2, we can easily verify that when $q_{1TC2} = g(y_1^*)$, $Det[J_{E_2}] = 0$, which means that $Det[J_{E_2}]$ has a zero eigenvalue $\lambda_1 = 0$. Letting $V = (v_1, v_2)^T$, $W = (w_1, w_2)^T$ be the eigenvectors of J_{E_2} and $J_{E_2{}^T}$ corresponding to the zero eigenvalue λ_1 respectively, then we can count out

$$V = \begin{pmatrix} v_1 \\ v_2 \end{pmatrix} = \begin{pmatrix} 1 \\ 0 \end{pmatrix}, \qquad W = \begin{pmatrix} w_1 \\ w_2 \end{pmatrix} = \begin{pmatrix} 1 \\ 0 \end{pmatrix}.$$

Moreover, we have

$$F_{q_1}(E_2; q_{1TC2}) = \begin{pmatrix} -mEx \\ 0 \end{pmatrix}_{(E_2;q_{1TC2})} = \begin{pmatrix} 0 \\ 0 \end{pmatrix},$$

$$DF_{q_1}(E_2; q_{1TC2})V = \begin{pmatrix} -mE & 0 \\ 0 & 0 \end{pmatrix}\begin{pmatrix} 1 \\ 0 \end{pmatrix}_{(E_2;q_{1TC2})} = \begin{pmatrix} -mE \\ 0 \end{pmatrix},$$

$$D^2F(E_2; q_{1TC2})(V, V) = \begin{pmatrix} \frac{\partial^2 F_1}{\partial x^2}{v_1}^2 + \frac{\partial^2 F_1}{\partial xy}v_1v_2 + \frac{\partial^2 F_1}{\partial y^2}{v_2}^2 \\ \frac{\partial^2 F_2}{\partial x^2}{v_1}^2 + \frac{\partial^2 F_2}{\partial xy}v_1v_2 + \frac{\partial^2 F_2}{\partial y^2}{v_2}^2 \end{pmatrix}_{(E_2;q_{1TC2})} = \begin{pmatrix} -2b_1 \\ 0 \end{pmatrix}.$$

Using these expressions, we can get

$$W^T F_{q_1}(E_2; q_{1TC2}) = 0,$$

$$W^T[DF_{q_1}(E_2; q_{1TC2})V] = -mE \neq 0,$$

$$W^T[D^2F(E_0; q_{1TC2})(V, V)] = -2b_1 \neq 0.$$

Hence from Sotomayor's theorem, the model (2.1) undergoes a transcritical bifurcation around the equilibrium point E_2 as the value of parameter q_1 passes through the critical threshold $q_1 = q_{1TC2}$. This completely ends the proof.

3.3. Global dynamics

In this section, we will further investigate the global dynamics of the model (2.1), and give the following result.

3.3.1. The dynamics near infinity

Now we discuss the qualitative properties of equilibrium point at infinity to study the global dynamics of the model (2.1), which can help us learn the behavior of orbits when either x or y is large. Firstly, we use the Poincar*é* transformation [62] $x = \frac{1}{z}$, $y = \frac{w}{z}$, to transform the model (2.1) into

$$\begin{cases} \frac{dw}{ds} = \frac{a_2w^2z}{uz+w} - \frac{b_2w^3}{uz+w} + \frac{cw^2z^2}{dz^2+w^2} - a_1wz + b_1w + (q_1 - q_2)mEwz, \\ \frac{dz}{ds} = \frac{cwz^3}{dz^2+w^2} + b_1z - a_1z^2 + q_1mEz^2, \end{cases} \tag{5.1}$$

where $ds = dt/z$. Then, it can see that, in the nonnegative w-axis, the model (5.1) has a unique equilibrium point $A(\frac{b_1}{b_2}, 0)$ in the first quadrant of $w - z$ plane.

Then by another Poincar*é* transformation $x = \frac{v}{z}$, $y = \frac{1}{z}$, the model (2.1) can be changed into

$$\begin{cases} \frac{dv}{ds} = \frac{b_2v}{uz+1} - \frac{a_2vz}{uz+1} - \frac{cvz^2}{dz^2+1} + a_1vz - b_1v^2 + (q_2 - q_1)mEvz, \\ \frac{dz}{ds} = \frac{b_2z}{uz+1} - \frac{a_2z^2}{uz+1} + q_2mEz^2, \end{cases} \tag{5.2}$$

where $ds = dt/z$. Now, we just need to discuss the equilibrium point $B(0, 0)$ of the model (5.2) in the first quadrant of $v - z$ plane.

Next, we analysis the qualitative properties of $A(\frac{b_1}{b_2}, 0)$ of the model (5.1) and $B(0, 0)$ of the model (5.2), and obtain the following Theorem.

Theorem 10. The model (5.1) has a unique equilibrium point $A(\frac{b_1}{b_2}, 0)$, where A is a saddle, and the model (5.2) has an equilibrium point $B(0, 0)$, which is an unstable node.

Proof: From the above analysis, the Jacobian matrix of the model (5.1) evaluated at $A(\frac{b_1}{b_2}, 0)$ is given by

$$J_A = \begin{pmatrix} -b_1 & (q_1 mE - q_2 mE - a_1 + a_2 + b_2 u)\frac{b_1}{b_2} \\ 0 & b_1 \end{pmatrix}.$$

Apparently, the eigenvalues of J_A are $\lambda_1 = -b_1 < 0$ and $\lambda_2 = b_1 > 0$. Hence, A is a saddle.

Similarly, the Jacobian matrix of the model (5.2) evaluated at $B(0, 0)$ is given by

$$J_B = \begin{pmatrix} b_2 & 0 \\ 0 & b_2 \end{pmatrix}.$$

We can easily see that the eigenvalues of J_B are $\lambda_1 = b_2 > 0$ and $\lambda_2 = b_2 > 0$. Hence, B is an unstable node. The proof of this theorem is completed.

3.3.2. Nonexistence of closed orbits

In this section, we will discuss whether the model (2.1) has closed orbits. In order to study this, we divide the whole parameter plane $(a_1, a_2, b_1, b_2, q_1, q_1, c, d, m, E, u) \in R_+^{11}$ into five regions as follows:

$$\begin{aligned}
S_1 &= S_{11} \cup S_{12} \cup S_{13} \cup S_{14} \cup S_{15} \cup S_{16}, \\
S_2 &= ((a_1, a_2, b_1, b_2, q_1, q_1, c, d, m, E, u) \in R_+^{11}; m = m_1, 0 < q_1 < g(y_3^*)), \\
S_3 &= ((a_1, a_2, b_1, b_2, q_1, q_1, c, d, m, E, u) \in R_+^{11}; 0 < m < m_1, 0 < q_1 < \min\{g(y_1^*), g(y_2^*)\}), \\
S_4 &= ((a_1, a_2, b_1, b_2, q_1, q_1, c, d, m, E, u) \in R_+^{11}; 0 < m < m_1, g(y_1^*) > g(y_2^*), g(y_2^*) \le q_1 < g(y_1^*)), \\
S_5 &= ((a_1, a_2, b_1, b_2, q_1, q_1, c, d, m, E, u) \in R_+^{11}; 0 < m < m_1, g(y_1^*) < g(y_2^*), g(y_1^*) \le q_1 < g(y_2^*)),
\end{aligned}$$

where

$$\begin{aligned}
S_{11} &= ((a_1, a_2, b_1, b_2, q_1, q_1, c, d, m, E, u) \in R_+^{11}; m > m_1, q_1 \ge \frac{a_1}{mE}), \\
S_{12} &= ((a_1, a_2, b_1, b_2, q_1, q_1, c, d, m, E, u) \in R_+^{11}; m > m_1, 0 < q_1 < \frac{a_1}{mE}), \\
S_{13} &= ((a_1, a_2, b_1, b_2, q_1, q_1, c, d, m, E, u) \in R_+^{11}; m = m_1, q_1 \ge \frac{a_1}{mE}), \\
S_{14} &= ((a_1, a_2, b_1, b_2, q_1, q_1, c, d, m, E, u) \in R_+^{11}; m = m_1, g(y_3^*) < q_1 < \frac{a_1}{mE}), \\
S_{15} &= ((a_1, a_2, b_1, b_2, q_1, q_1, c, d, m, E, u) \in R_+^{11}; 0 < m < m_1, q_1 \ge \frac{a_1}{mE}), \\
S_{16} &= ((a_1, a_2, b_1, b_2, q_1, q_1, c, d, m, E, u) \in R_+^{11}; 0 < m < m_1, \max\{g(y_1^*), g(y_2^*)\} \le q_1 < \frac{a_1}{mE}).
\end{aligned}$$

Then we can get the following result.

Theorem 11. The model (2.1) has no closed orbit.

Proof: We firstly consider $(a_1, a_2, b_1, b_2, q_1, q_1, c, d, m, E, u) \in S_1$. From previous analysis, we know that the model (2.1) has no interior equilibrium point in S_1, then the model (2.1) has no closed orbit because $x = 0, y = 0$ and $y = y_3^*$ are invariant sets, otherwise, the closed orbit must intersect with one of these three orbits. Now we consider $(a_1, a_2, b_1, b_2, q_1, q_1, c, d, m, E, u) \in S_2$, it can claim that there is no closed orbit in S_2. Indeed, supposing that the model (2.1) exists a closed orbit, then there is an equilibrium point in the interior of the closed orbit. Since $y = y_3^*$ is an invariant set and the interior equilibrium point E_3^* lies on this line, hence the closed orbit must have two intersection points with $y = y_3^*$. This contradicts the existence and uniqueness of solutions. A similar argument, because $y = y_1^*$ and $y = y_2^*$ are also invariant sets, thus the proof of the case that $(a_1, a_2, b_1, b_2, q_1, q_1, c, d, m, E, u) \in S_3$ *or* S_4 *or* S_5 is similar to that of S_2. Hence the model (2.1) has no closed orbits. This completely ends the proof.

According to the above mathematical analysis, some key threshold conditions have been derived to guarantee the existence and stability of all possible equilibrium points, the occurrence of saddle-node bifurcation and transcritical bifurcation, nonexistence of closed orbit, which can provide a theoretical basis for numerical simulation about dynamical behaviors of the model (2.1). Furthermore, it is worthy of our attention from the given related theorems that the parameter m and q_1 can be regarded as key parameter to control dynamic evolution process of the model (2.1).

4. Results of numerical simulations

As we all know, Allee effect and harvest have a serious influence on the dynamic behavior of the model (2.1). In order to explore their influence mechanism and the inhibition of algicidal bacteria on algae, some numerical simulation works are carried out with the help of MATLAB software, which also in turn verify the correctness and feasibility of the theoretical results. Furthermore, some phase diagrams (see Figure 2, Figure 3, Figure 4 and Figure 5) can represent the survival mode of algicidal bacteria and algae, and bifurcation diagrams (see Figure 1) can represent the dynamic change process of algae inhibition by algicidal bacteria with the change of key ecological and environmental factors.

It is easy to find from table 1 that the model (2.1) has two boundary equilibrium points E_2 and E_3 when $0 < m < m_1$, further when $0 < q_1 < \min\{g(y_1^*), g(y_2^*)\}$, the model(2.1) has two interior equilibrium points E_1^* and E_2^*, hence the premise of parametric ranges are $0 < m < m_1$ in Figure 1(a) and $0 < q_1 < \min\{g(y_1^*), g(y_2^*)\}$ in Figure 1(b). Furthermore, it is worth emphasizing that in Figure 1(a) the three vertical lines passing through points $(\frac{a_1}{mE}, 0)$, $(g(y_1^*), 0)$ and $(g(y_2^*), 0)(g(y_1^*) < g(y_2^*))$ are the transcritical bifurcation lines TC_1 and TC_2 as well as a critical threshold line CT, respectively. Moreover, if $q_1 < \min\{g(y_1^*), g(y_2^*)\}$), which means that the model (2.1) has two interior equilibrium points E_1^* and E_2^*, and four boundary equilibrium points E_0, E_1, E_2 and E_3 when the value of q_1 is positioned within region I of Figure 1(a), where E_2^*, E_0 and E_2 are saddle, E_1^* and E_1 are stable node and E_3 is an unstable node, the corresponding phase diagram is shown in Figure 2(a). Now it is worth pointing out that the equilibrium point E_1^* is a stable node, which suggests that algae and algicidal bacteria can form a stable coexistence regional mode, but E_1 is a stable node, which also suggests that algicidal bacteria will eventually go extinct if the density of algicidal bacteria is below a critical threshold. Thus, this result is in response to the Allee effect, and further reveals the influence mechanism of Allee effect on the dynamic change of algae and algicidal bacteria. That is to say, if the

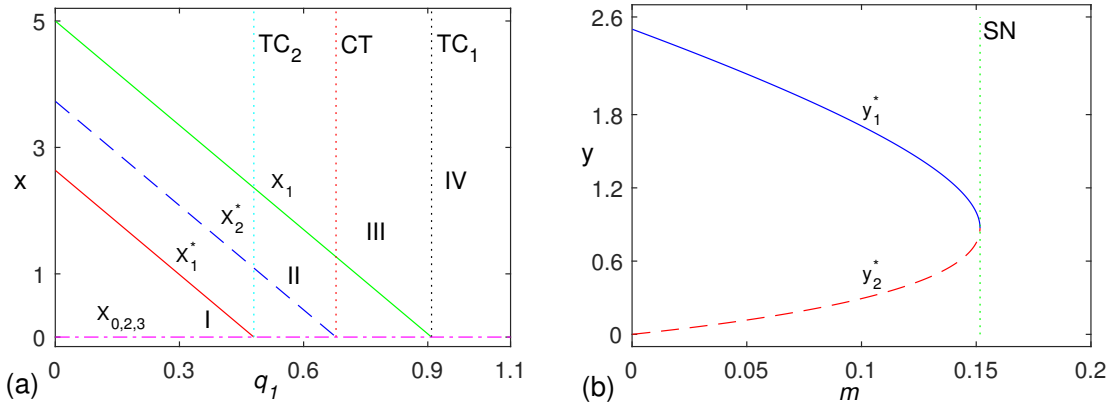

Figure 1. Bifurcation diagram of the model (2.1) in the $x-q_1$ and $y-m$ plane constructed for $a_1 = 0.5, a_2 = 0.5, b_1 = 0.1, b_2 = 0.2, c = 0.6, u = 1, E = 5, q_2 = 0.2$, (a) $d = 0.4, m = 0.11$; (b) $d = 1.5, q_1 = 0.2$. Three diagonal lines stand for two interior equilibrium points: E_1^*(red), E_2^*(blue), and a boundary equilibrium point E_1(green). What's more, red horizontal dashed dotted line indicates three boundary equilibrium point: E_0, E_2, E_3, the detailed analysis is explained in the text. The solid and dashed lines indicate equilibrium point in stable and unstable state, respectively.

Allee effect threshold is too small and algicidal bacteria can not reproduce rapidly, the algal population will reproduce in large numbers, which can increase the possibility of algal bloom.

While when the value of key parameter q_1 is gradually increasing across the transcritical bifurcation TC_2 and enters into region II, there is a unique interior equilibrium point E_2^* and four boundary equilibrium points E_0, E_1, E_2 and E_3 in the model (2.1), where E_2^* and E_0 are saddle, E_1 and E_2 are stable node and E_3 is an unstable node, the corresponding phase diagram is shown in Figure 2(b). Thus, it should be pointed out by us that E_1 and E_2 are stable node, which hints that algicidal bacteria will eventually go extinct if the density of algicidal bacteria is below a critical threshold, but algae will eventually go extinct if the density of algicidal bacteria is greater than the critical threshold, these results reveal that algae and algicidal bacteria can not form a stable coexistence mode under the joint action of Allee effect and harvest. As the value of key parameter q_1 gradually increases across the critical threshold line CT and enters into region III, there is no interior equilibrium point and only four boundary equilibrium points E_0, E_1, E_2 and E_3 in the model (2.1), where E_0 and E_3 are saddle, E_1 and E_2 are stable node, the corresponding phase diagram is shown in Figure 2(c). It is obvious to find by comparing Figure 2b with Figure 2c that algae and algicidal bacteria still can not form a stable coexistence mode under the joint action of Allee effect and harvest, but their influences have always existed. When the value of key parameter q_1 continuously increases across the transcritical bifurcation TC_1 and finally enters into region IV, there is no interior equilibrium point and only three boundary equilibrium points E_0, E_2 and E_3 in the model (2.1), where E_3 is a saddle, E_0 and E_2 are stable node, the corresponding phase diagram is shown in Figure 2(d), which suggests that if the density of algicidal bacteria is lower than a critical threshold, algicidal bacteria will become extinct, while algicidal bacteria can survive if the density of algicidal bacteria is higher than this critical threshold, but no matter what, algae is always going extinct. These results show that if the value of the harvesting parameter is too large, algae will go extinct, which is not conducive to the permanence of algae and algicidal bacteria.

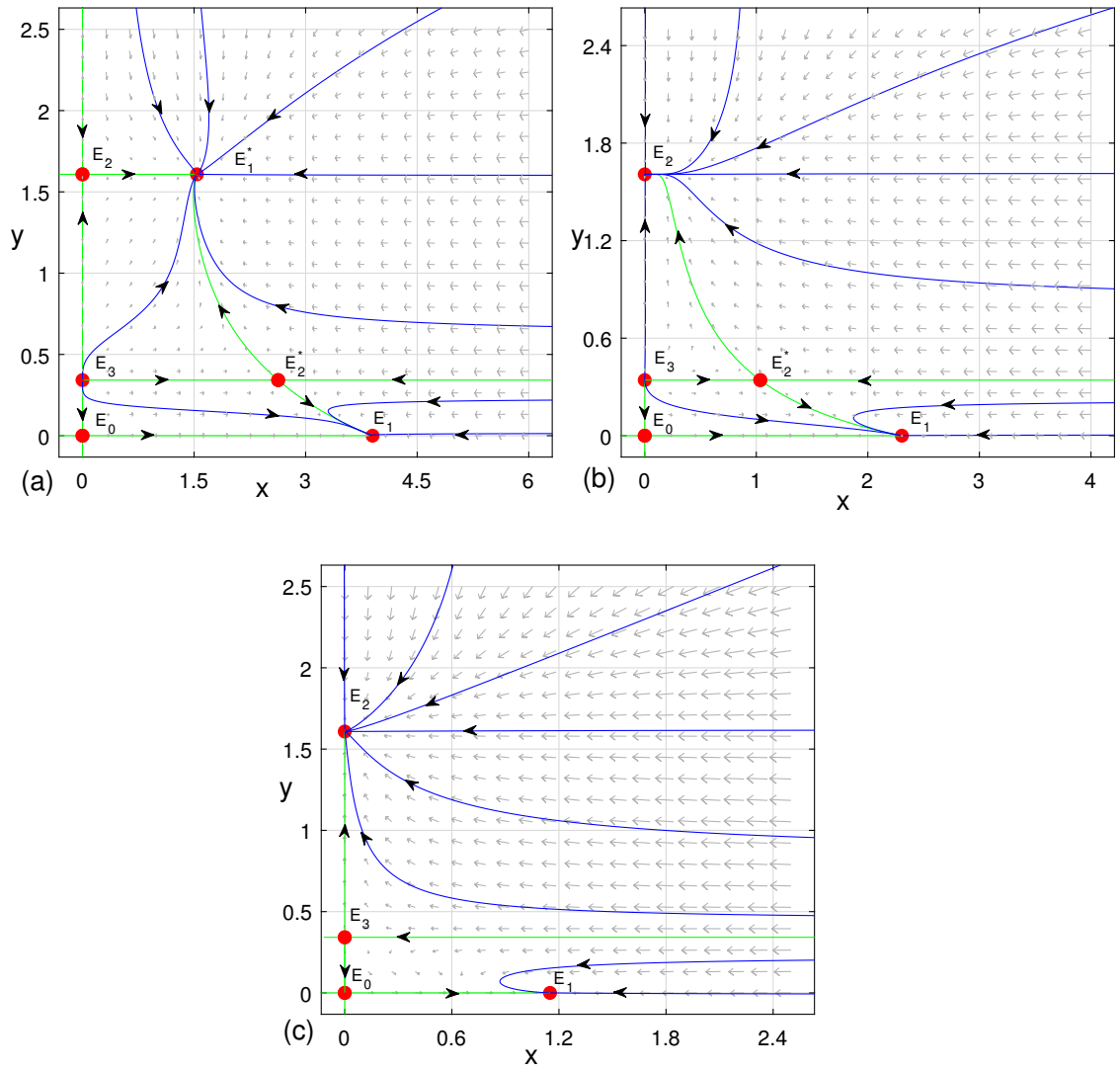

Figure 2. The phase portraits of the model (2.1) (varying with parameter q_1). The values of parameters are $a_1 = 0.5, a_2 = 0.5, b_1 = 0.1, b_2 = 0.2, c = 0.6, u = 1, E = 5, q_2 = 0.2$, $m = 0.11, d = 1.5$, and (a) $q_1 = 0.2$; (b) $q_1 = 0.49$; (c) $q_1 = 0.7$; (d) $q_1 = 0.92$. The horizontal axis indicates the first species x and the vertical axis indicates the second species y. The green curves are stable or unstable orbits; the red points are the equilibrium points.

In order to investigate the occurrence of the saddle-node bifurcation behavior in the model (2.1), a bifurcation diagram of the model (2.1) has been drawn by directly continuing the threshold value of m_{SN} in Figure 1(b), where the vertical lines passing through points $(m_1, 0)$ are the saddle-node bifurcation curve SN. If $0 < m < m_{SN}$ and $q_1 < \min\{g(y_1^*), g(y_2^*)\}$, then the model (2.1) has two interior equilibrium points E_1^* and E_2^* and four boundary equilibrium points E_0, E_1, E_2 and E_3 (see Figure 2(a)). If the value of m gradually increases and reaches m_{SN}, then the equilibrium point E_1^* and E_2^* can coincide at the line SN. Thus, the model (2.1) will produce the coincident point E_3^* when $q_1 < g(y_3^*)$, and three boundary equilibrium points E_0, E_1, E_4 still exist, where E_0 is a saddle, E_1 is a

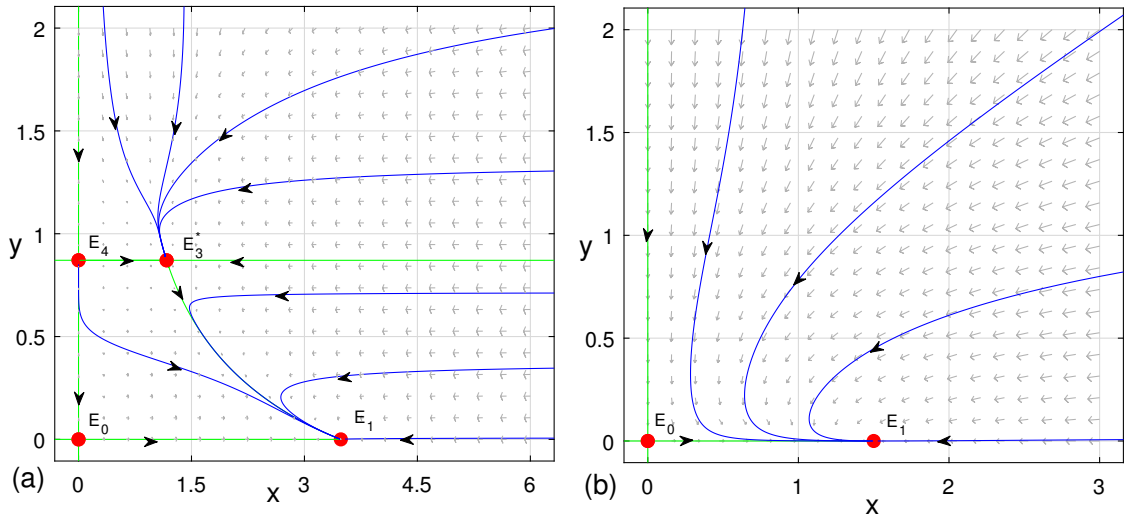

Figure 3. The phase portraits of the model (2.1) (varying with parameter m). The values of parameters are $a_1 = 0.5, a_2 = 0.5, b_1 = 0.1, b_2 = 0.2, c = 0.6, u = 1, E = 5, q_2 = 0.2, d = 1.5, q_1 = 0.2$, and (a) $m = 0.1516685226$; (b) $m = 0.35$.

stable node and E_3^* and E_4 are saddle-node points, the corresponding phase diagram is shown in Figure 3(a). However when the value of m continuously increases and acroses the threshold value m_{SN}, the model (2.1) has no interior equilibrium point and two boundary equilibrium points E_0 and E_1 still exist, where E_0 is a saddle, E_1 is a stable node, the corresponding phase diagram is shown in Figure 3(b). Therefore, it is worthwhile to be happy from Figure 2a, Figure 3a and Figure 3b that the model (2.1) have formed saddle-node bifurcation, that is to say, if the value of the fraction m of the stock available for harvesting is lower than the key value m_{SN}, then algae and algicidal bacteria can form a stable coexistence regional mode when the density of algicidal bacteria is higher than a critical threshold, but if the value of the fraction m of the stock available for harvesting is higher than the key value m_{SN}, algicidal bacteria always going extinct no matter what the density of algicidal bacteria is.

Furthermore, in order to explore the interaction mechanism of harvesting related parameters m and q_1 on the permanence of algae and algicidal bacteria, some phase portraits of the model have been given. When $m = m_{SN} = 0.1516685226$, if $q_1 = 0.48$, then the model (2.1) has no interior equilibrium point and three boundary equilibrium points E_0, E_1 and E_4 exist, where E_0 is a saddle, E_1 is a stable node and E_4 is a saddle-node point, which is shown in Figure 4(a). It is obvious to know from Figure 4(a) that if the density of algicidal bacteria is lower than a critical threshold, algicidal bacteria will become extinct, but algae can survive, while algicidal bacteria can survive if the density of algicidal bacteria is higher than this critical threshold, but algae will go extinct. If $q_1 = 0.67$, then the model (2.1) has no interior equilibrium point and two boundary equilibrium points E_0 and E_4 exist, where E_0 is a stable node and E_4 is a saddle-node point, which is shown in Figure 4(b). It is easy to find that the density of algicidal bacteria is lower than a critical threshold, algae and algicidal bacteria will become extinct together, while algicidal bacteria can survive if the density of algicidal bacteria is higher than this critical threshold, but algae will become extinct. But it is worth emphasizing that the persistence and extinction of algicidal bacteria can reveal the existence of Allee effect. However, it is a pity that

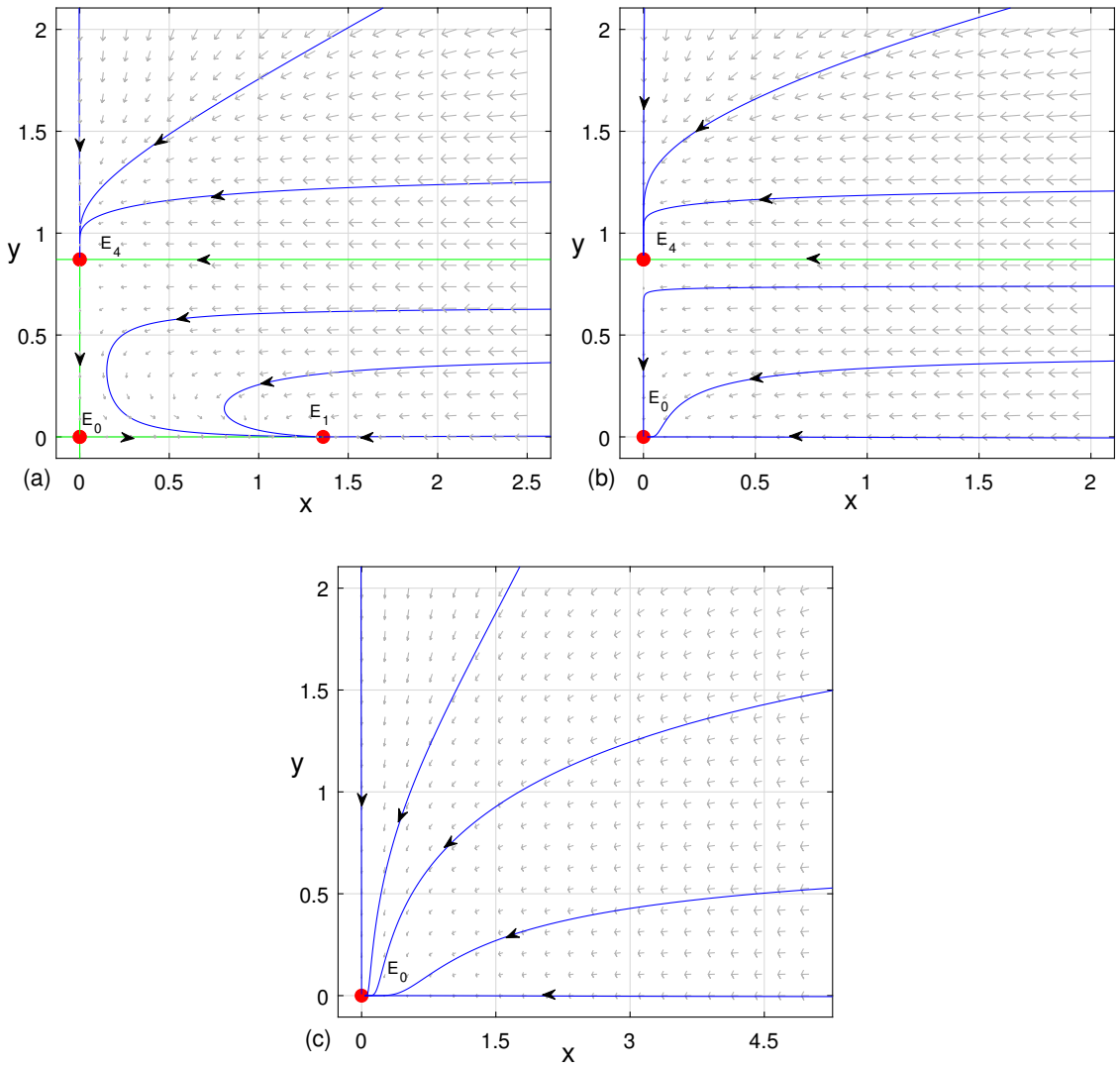

Figure 4. The phase portraits of the model (2.1) (varying with parameter q_1 and m). The values of parameters are $a_1 = 0.5, a_2 = 0.5, b_1 = 0.1, b_2 = 0.2, c = 0.6, u = 1, E = 5, q_2 = 0.2, d = 1.5$, and (a) $m = 0.1516685226, q_1 = 0.48$; (b) $m = 0.1516685226, q_1 = 0.67$; (c) $m = 0.35, q_1 = 0.3$.

when $m = 0.35$ and $q_1 = 0.3$, the model (2.1) only has one boundary equilibrium point E_0, which is a stable node, which is shown in Figure 4(c), and this suggests that when the overall harvest is excessive, algae and algicidal bacteria will eventually go extinct regardless of their initial density. In addition, we also investigate the impact of Allee effect on amensalism ecosystem by comparing Figure 2(a) and Figure 5 with different u values, it is easy to find that the strength of Allee effect does not change the type and stability of equilibrium points, and only affects the internal dynamic evolution characteristics of algae and algicidal bacteria. In other words, it only affects the survival and reproduction of algicidal bacteria.

Based on the above dynamic analysis results, we will reveal biological significance of the dynamic

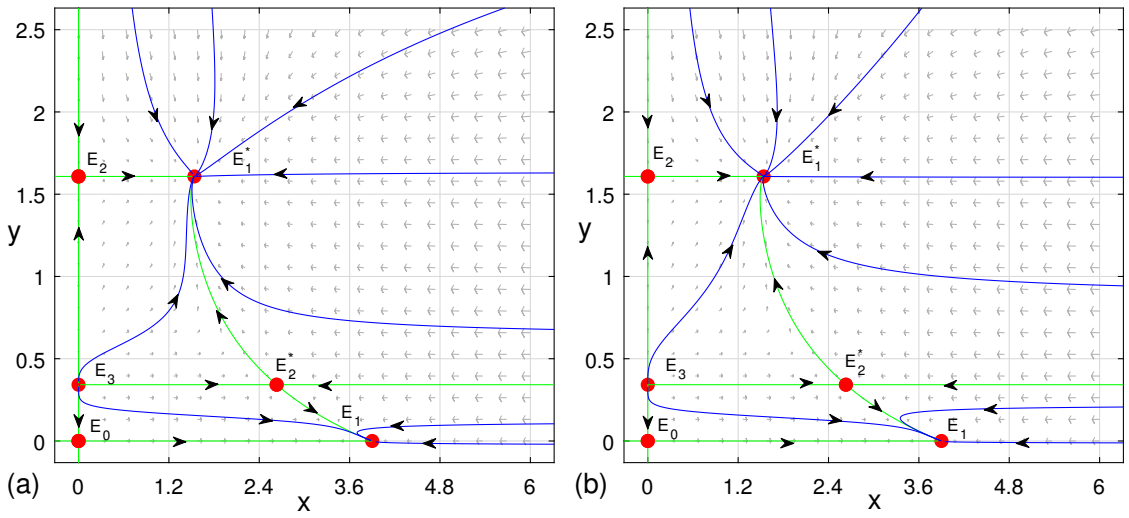

Figure 5. The phase portraits of the model (2.1) (varying with parameter u). The values of parameters are $a_1 = 0.5, a_2 = 0.5, b_1 = 0.1, b_2 = 0.2, c = 0.6, E = 5, m = 0.11, q_1 = 0.11, q_2 = 0.2, d = 1.5$, and (a) $u = 0.5$; (b) $u = 1.5$.

behavior of the model (2.1). Firstly, it is easy to find from Figure 2 that the key threshold of Allee effect on algicidal bacteria has always been the y coordinate value of the equilibrium point E_3, if the density of algicidal bacteria is lower than the critical value, then algicidal bacteria is always going extinct, if the density of algicidal bacteria is larger than the critical value, then algicidal bacteria always approaches to the y coordinate value of equilibrium point E_2. That is to say, the initial density of algicidal bacteria determines whether algicidal bacteria can survive for a long time, and then affects whether algae and algicidal bacteria can coexist for a long time. However, it is a pity to find from Figure 5 that Allee effect has little effect on the specific dynamic behavior of the model (2.1), and does not change the dynamic characteristics of the model (2.1). Secondly, it is worthy of our attention from Figure 2(a), Figure 3 and Figure 4 that if the comprehensive harvest is moderate ($m < m_{SN}$ and $q_1 < \min\{g(y_1^*), g(y_2^*), g(y_3^*)\}$), then algae and algicidal bacteria can form a stable coexistence regional mode, which can be produced by saddle-node bifurcation, it stands for new stable and orderly formation. In other words, saddle-node bifurcation can lead to the coexistence of algae and algicidal bacteria, which is conducive to a good cycle of biological control of algae. However, if we over harvest or salvage algae, although we can effectively control the outbreak of algal bloom, but we also indirectly harvest or salvage a part of algicidal bacteria, which is not conducive to the rapid propagation and space survival of algicidal bacteria and can lead to the reproduce failure and the extinction of algicidal bacteria. Finally, it should be stressed from Figure 1(a) and Figure 2 that the model (2.1) can appear transcritical bifurcation, which can represent steady state transformation, that is to say, the intrinsic nature of amensalism dynamic relationship has not been changed, but only the coexistence mode of algae and algicidal bacteria has been changed. Moreover, all the numerical simulation results also indirectly prove the validity and feasibility of the theoretical results.

5. Conclusion

In this paper, with the framework of studying how algicidal bacteria inhibit algal growth, we have proposed an aquatic amensalism model with a non-selective harvesting and Allee effect, Using relevant mathematical theory, we mainly gave some critical conditions for the existence and local stability of all possible equilibrium points and the occurrence of saddle-node bifurcation and transcritical bifurcation. Furthermore, the dynamics near infinity and nonexistence of closed orbits have also been probed. These theoretical results not only provide theoretical basis for numerical simulation, but also suggest that the model (2.1) has some equilibrium points of different properties and bifurcation dynamics.

In order to investigate how harvest and Allee effect affect the dynamic behavior of the aquatic amensalism model(2.1), some numerical simulation works have been carried out, which can not only make clear the feasibility of mathematical deduction results, but also reveal the dynamic trend of algae and algicidal bacteria, and is more able to show the changing characteristics of attributes and types of equilibrium points. The numerical simulation results show that the model (2.1) has different types of equilibrium points with the value of key parameter q_1 changing, which also can produce transcritical bifurcation. At the same time, as the value of key parameter q_1 increases, algae and algicidal bacteria have different coexistence modes, such regional stable state mode, algicidal bacteria gradual extinction mode and algae gradual extinction mode. Meanwhile, it is also worth explaining that the model (2.1) can generate saddle-node bifurcation dynamics, which mainly represents a new stable and orderly formation with the value of key parameter m changing, and hints that algae and algicidal bacteria can survive with a stable manner in a certain range. Furthermore, it should be stressed that non-selective harvesting can strongly affect the survival and extinction of algae and algicidal bacteria, and over harvesting can eliminate the Allee effect on the dynamic behavior of the model (2.1). However, it needs our special emphasis that the Allee effect of algicidal bacteria is the key factor whether algicidal bacteria can effectively inhibit the growth of algae population.

Compared with the previous research on some amensalism models, the greatest advantage of this paper is to establish an aquatic amensalism model from the perspective of exploratory research on biological algae control technology, which can put the amensalism model into a certain ecological environment system, and make that the bifurcation dynamic behaviors have certain ecological and environmental significance. On this basis, the inhibition mechanism of algicidal bacteria on algae is explored from the perspective of population dynamics, which can not only explain the internal ecological significance of bifurcation dynamics, but also help us to deeply understand the algae dissolving mode and mechanism of algicidal bacteria.

In the follow-up research works, we will first deepen theoretical research of bifurcation dynamics, especially Bogdanov-Takens bifurcation, and then further modify the model to study the growth trend of algae population dynamics when the inhibitory effect of algicidal bacteria on algae is at a disadvantage, finally explore how to effectively repair the microbial flora structure and enhance the inhibitory ability of algicidal bacteria, which can effectively prevent the outbreak of algal bloom and maintain the basic ecological balance of water body. In a word, all these results are expected to be useful in studying dynamic behavior of the amensalism ecosystem and algae controlling technology by microorganism.

Acknowledgments

This work was supported by the key International Cooperation Projects of China (Grant No: 2018YFE0103700), the National Natural Science Foundation of China (Grant No: 31570364, 61871293, 41876124, 61901303), by the Zhejiang Provincial Natural Science Foundation of China (Grant No: 2Q18C030002), by key research and development projects of Zhejiang Province (Grant No: 2021C03166), by the Science and Technology program of Cangnan, China (Grant No: 2018ZG29), by Science and Technology Major Program of Wenzhou, China (Grant No: 2018ZG002).

Conflict of interest

The author declares that there are no conflicts of interest.

References

1. T. F. Steppe, J. B. Olson, H. W. Paerl, Consortial N2 fixation: A strategy for meeting nitrogen requirements of marine and terrestrial cyanobacterial mats, *FEMS. Microbiol. Ecol.*, **21** (1996), 149–156.
2. A. Dakhama, J. Noue, M. C. Lavoie, Isolation and identification of antialgal substances produced by Pseudomonas aeruginosa, *J. Appl. Phycol.*, **5** (1993), 297–306.
3. Y. Kawano, Y. Nagawa, H. Nakanishi, H. Nakajima, M. Matsuo, T. Higashihara, Production of thiotropocin by a marine bacterium Caulobacter sp and its antimicroalgal activities, *J. Mar. Biotechnol.*, **5** (1997), 225–229.
4. C. Q. Xiao, H. Jiang, K. Cheng, Y. J. Zhao, Selection of algae lysing actinomycetes AN02 and optimization of its cultural conditions, *J. Microbiol.*, **27** (2007), 11–14.
5. H. J. Choi, B. H. Baik, J. D. Kim, M. S. Han, Streptomyces neyagawaensis as a control for the hazardous biomass of Microcystis aeruginosa (Cyanobacteria) in eutrophic freshwaters, *Biol. Control.*, **33** (2005), 335–343.
6. Y. F. Yang, X. J. Hu, J. Zhang, Y. X. Gong, Community level physiological study of algicidal bacteria in the phycospheres of Skeletonema costatum and Scrippsiella trochoidea, *Harmful. Algae.*, **28** (2013), 88–96.
7. E. Odum, *Fundamentals of ecology*, Saunders, Philadelphia, 1953.
8. J. Li, *Ecology*, Science Press, 2014.
9. G. C. Sun, Qualitative analysis on two populations amensalism model, *J. Jiamusi Univ.*, **21** (2003), 283–286.
10. Z. F. Zhu, Q. L. Chen, Mathematic analysis on commensalism Lotka-Volterra model of populations, *J. Jixi. Univ.*, **8** (2008), 100–101.
11. F. D. Chen, W. X. He, R. Y. Han, On discrete amensalism model of Lotka-Volterra, *J. Beihua. Univ.*, **16** (2015), 141–144.
12. H. H. Xiong, B. B. Wang, H. L. Zhang, Stability analysis on the dynamic model of fish swarm amensalism, *Adv. Appl. Math.*, **5** (2016), 255–261.

13. R. X. Wu, A two species amensalism model with non-monotonic functional response, *Commun. Math. Biol. Neurosci.*, **2016** (2016), 19.

14. X. Y. Guan, F. D. Chen, Dynamical analysis of a two species amensalism model with Beddington-DeAngelis functional response and Allee effect on the second species, *Nonlinear. Anal. RWA.*, **48** (2019), 71–93.

15. L. C. Zhao, Q. L. Zhang, Q. C. Yang, The induction control of a three-species model with partial harm relations, *J. Biomath.*, **20** (2005), 37–42.

16. R. X.Wu, L. Li, Q. F. Lin, A Holling type commensal symbiosis model involving Allee effect, *Commun. Math. Biol. Neurosci.*, **2018** (2018), 6.

17. Q. Q. Su, F. D. Chen, The influence of partial closure for the populations to a non-selective harvesting Lotka-Volterra discrete amensalism model, *Adv. Differ. Equ-Ny.*, **2019** (2019), 281.

18. R. Y. Han, Y. L. Xue, L. Y. Yang, F. D. Chen, On the existence of positive periodic solution of a Lotka-Volterra amensalism model, *J. Longyan. Univ.*, **33** (2015), 22–26.

19. Z. Wei, Y. H. Xia, T. H. Zhang, Stability and bifurcation analysis of an amensalism model with weak Allee effect, *Qual. Theor. Dyn. Syst.*, **19** (2020), 23.

20. F. Courchamp, L. Berec, J. Gascoigne, *Allee effects in ecology and conservation*, Oxford University Press, New York, 2008.

21. W. C. Allee, *Animal aggragations, a study in general sociology*, University of Chicago Press, Chicago, 1931.

22. P. A. Stephens, W. J. Sutherland, Consequences of the Allee effect for behavior, ecology and conservation, *Trends. Ecol. Evol.*, **14** (1999), 401–405.

23. F. Courchamp, T. Clutton-Brock, B. Grenfell, Inverse density dependence and the Allee effect, *Trends. Ecol. Evol.*, **14** (1999), 405–410.

24. P. A. Stephens, W. J. Sutherland, R. P. Freckleton, What is the Allee effect?, *Oikos*, **87** (1999), 185–190.

25. M. Liermann, R. Hilborn, Depensation: Evidence, models and implication, *Fish Fish.*, **2** (2001), 33–58.

26. G. P. Stamou, M. D. Asikidis, The effect of density on the demographic parameters of two oribatid mites, *Rev. Ecol. Biol. Sology.*, **26** (1989), 321–330.

27. F. Courchamp, L. Berec, J. Gascoigne, *Allee effects in ecology and conservation*, Oxford University Press, New York, 2008.

28. C. Rebelo, C. Soresina, Coexistence in seasonally varying predator-prey systems with Allee effect, *Nonlinear Anal. RWA*, **55** (2020),103140.

29. U. Kumar, P. S. Mandal, E. Venturino, Impact of Allee effect on an eco-epidemiological system, *Ecol. Complex.*, **42** (2020), 100828.

30. D. Sen, S. Ghorai, S. Sharma, M. Banerjee, Allee effect in prey growth reduces the dynamical complexity in prey-predator model with generalist predator, *Appl. Math. Model.*, **91** (2021), 768–790.

31. D. Y. Bai, Y. Kang, S. G. Ruan, L. S. Wang, Dynamics of an intraguild predator food web model with strong Allee effect in the basal prey, *Nonlinear Anal. RWA*, **58** (2021), 103206.
32. J. P. Tripathi, P. S. Mandal, A. Poonia, V. P. Bajiya, A widespread interaction between generalist and specialist enemies: The role of intraguild predation and Allee effect, *Appl. Math. Model.*, **89** (2021), 105–135.
33. P. G. Brown, P. Timmerman, *Ecological Economics for the Anthropocene: An Emerging Paradigm*, Columbia University Press, United States, 2015.
34. T. K. Ang, H. M. Safuan, Dynamical behaviors and optimal harvesting of an intraguild prey-predator fishery model with Michaelis-Menten type predator harvesting, *BioSystems*, **202** (2021), 104357.
35. C. W. Clark, Mathematical models in the economics of renewable resources, *SIAM Rev.*, **21** (1979), 81–99.
36. C. W. Clark, M. Mangel, Aggregation and fishery dynamics: A theoretical study of schooling and the purse seine tuna fisheries, *Fish. B-Noaa.*, **77** (1979), 317–337.
37. T. Das, R. N. Mukherjee, K. S. Chaudhuri, Harvesting of a prey-predator fishery in the presence of toxicity, *Appl. Math. Model.*, **33** (2009), 2282–2292.
38. T. Das, R. N. Mukherjee, K. S. Chaudhuri, Bio-economic harvesting of a prey-predator fishery, *J. Biol. Dynam.*, **3** (2009), 447–462.
39. X. X. Liu, Q. D. Huang, Analysis of optimal harvesting of a predator-prey model with Holling type IV functional response, *Ecol. Complex.*, **42** (2020), 100816.
40. E. Bellier, B. E. Sether, S. Engen, Sustainable strategies for harvesting predators and prey in a fluctuating environment, *Ecol. Model.*, **440** (2021), 109350.
41. J. Datta, D. Jana, R. K. Upadhyay, Bifurcation and bio-economic analysis of a prey-generalist predator model with Holling type IV functional response and nonlinear age-selective prey harvesting, *Chaos Soliton. Fract.*, **122** (2019), 229–235.
42. M. Li, B. S. Chen, H. W. Ye, A bioeconomic differential algebraic predator-prey model with nonlinear prey harvesting, *Appl. Math. Model.*, **42** (2017), 17–28.
43. R. P. Gupta, P. Chandra, M. Banerjee, Dynamical complexity of a prey-predator model with nonlinear predator harvesting, *Discrete. Cont. Dyn-B.*, **20** (2015), 423–443.
44. L. N. Guin, S. Pal, S. Chakravarty, S. Djilali, Pattern dynamics of a reaction-diffusion predator-prey system with both refuge and harvesting, *Int. J. Biomath.*, **14** (2020), 2050084.
45. L. N. Guin, R. Murmu, H. Baek, K. H. Kim, Dynamical analysis of a Beddington-DeAngelis interacting species system with prey harvesting, *Math. Probl. Eng.*, **2020** (2020), 22.
46. L. N. Guin, S. Acharya, Dynamic behaviour of a reaction-diffusion predator-prey model with both refuge and harvesting, *Nonlinear Dynam.*, **88** (2017), 1–33.
47. H. G. Yu, M. Zhao, R. P. Agarwal, Stability and dynamics analysis of time delayed eutrophication ecological model based upon the Zeya reservoir, *Math. Comput. Simulat.*, **97** (2014), 53–67.
48. L. V. Bertalanffy, *Theoretische biologise*, Berlin, 1932.

49. H. G. Yu, M. Zhao, Q, Wang, R. P. Agarwal, A focus on long-run sustainability of an impulsive switched eutrophication controlling system based upon the Zeya reservoir, *J. Franklin Inst.*, **351** (2014), 487–499.

50. H. Malchow, S. Petrovskii, A. Medvinsky, Pattern formation in models of plankton dynamics: A synthesis, *Oceanol. Acta.*, **24** (2011), 479–487.

51. D. Balram, K. Ankit, P. M. Atasi, Global stability and Hopf-bifurcation of prey-predator system with two discrete delays including habitat complexity and prey refuge, *Commun. Nonlinear Sci. Numer. Simulat.*, **67** (2019), 528–554.

52. L. N. Guin, E. Das, M. Sambath, Pattern formation scenario via Turing instability in interacting reaction-diffusion systems with both refuge and nonlinear harvesting, *J. Appl. Nonl. Dyn.*, **9** (2020), 1–21.

53. L. N. Guin, H. Baek, Comparative study between prey-dependent and ratio-dependent predator-prey models relating to patterning phenomenon, *Math. Comput. Simulat.*, **146** (2018), 100–117.

54. L. N. Guin, B. Mondal, S. Chakravarty, Spatiotemporal patterns of a pursuit-evasion generalist predator-prey model with prey harvesting, *J. Appl. Nonl. Dyn.*, **7** (2018), 165–177.

55. S. T. Wang, H. G. Yu, Complexity anaylsis of a modified predator-prey system with Beddington-DeAngelis functional response and Allee-like effect on predator, *Discrete Dyn. Na. Soc.*, **2021** (2021), 1–18.

56. X. X. Li, H. G. Yu, C. J. Dai, Z. L. Ma, Q. Wang, M. Zhao, Bifurcation analysis of a new aquatic ecological model with aggregation effect, *Math. Comput. Simulat.*, **190** (2021), 75–96.

57. R. J. Han, L. N. Guin, B. X. Dai, Cross-diffusion-driven pattern formation and selection in a modified Leslie-Gower predator-prey model with fear effect, *J. Biol. Syst.*, **28** (2020), 1–38.

58. R. J. Han, L. N. Guin, B. X. Dai, Consequences of refuge and diffusion in a spatiotemporal predator-prey model, *Nonlinear Anal. RWA.*, **60** (2021), 103311.

59. H. J. Guo, W. Zhang, X. M. Zhang, L. Q. Mao, W. Y. Zang, Process of alge-lysis and chlorophyll degradation kinetics of Microbacterium oleivoran bacteria, *Environ. Chem.*, **190** (2021), 75-96.

60. S. E. Jorgensen, G. Bendoricchio, *Fundamentals of Ecological Modelling*, Elsevier BV, The Netherlands, 2001.

61. D. P. Hu, H. J. Cao, Stability and bifurcation analysis in a predator-prey system with Michaelis-Menten type predator harvesting, *Nonlinear Anal. RWA.*, **33** (2017), 58–82.

62. Z. F. Zhang, W. Z. Huang, Z. X. Dong, *Qualitative Theory of Differential Equation*, Science Press, Beijing,1992.

63. L. Perko, *Differential Equations and Dynamical Systems*, Springer, New York, 2001.

Appendix

Table 1. Equilibrium points of system (1.4) in finite planes.

Qualifications			Location of equilibrium	stability
$m > m_1$	$q_1 > \frac{a_1}{mE}$		E_0	E_0 stable node;
	$q_1 = \frac{a_1}{mE}$		E_0	E_0 saddle-node;
	$0 < q_1 < \frac{a_1}{mE}$		E_0, E_1	E_0 saddle;E_1 stable node;
$m = m_1$	$q_1 > \frac{a_1}{mE}$		E_0, E_4	E_0 stable node; E_4 saddle-node;
	$q_1 = \frac{a_1}{mE}$		E_0, E_4	E_0,E_4 saddle-node;
	$g(y_3^*) < q_1 < \frac{a_1}{mE}$		E_0, E_1, E_4	E_0 saddle;E_1 stable node; E_4 saddle-node;
	$0 < q_1 < g(y_3^*)$		E_0, E_1, E_4, E_3^*	E_0 saddle; E_1 stable node; E_4,E_3^* saddle-node;
$0 < m < m_1$	$q_1 > \frac{a_1}{mE}$		E_0, E_2, E_3	E_0,E_2 stable node; E_3 saddle;
	$q_1 = \frac{a_1}{mE}$		E_0, E_2, E_3	E_0 saddle-node;E_2 stable node; E_3 saddle;
	$\max\{g(y_1^*), g(y_2^*)\} < q_1 < \frac{a_1}{mE}$		E_0, E_1, E_2, E_3	E_0, E_3 saddle;E_1, E_2 stable node;
	$0 < q_1 < \min\{g(y_1^*), g(y_2^*)\}$		$E_0, E_1, E_2, E_3, E_1^*, E_2^*$	E_0, E_2, E_2^* saddle; E_1, E_1^* stable node; E_3 unstable node;
	$g(y_1^*) > g(y_2^*)$	$q_1 = g(y_1^*)$	E_0, E_1, E_2, E_3	E_0, E_3 saddle;E_1 stable node; E_2 saddle-node;
		$q_1 = g(y_2^*)$	$E_0, E_1, E_2, E_3, E_1^*$	E_0, E_2 saddle;E_3 saddle-node; E_1, E_1^* stable node;
		$g(y_2^*) < q_1 < g(y_1^*)$	$E_0, E_1, E_2, E_3, E_1^*$	E_0, E_2, E_3 saddle; E_1, E_1^* stable node;
	$g(y_1^*) < g(y_2^*)$	$q_1 = g(y_2^*)$	E_0, E_1, E_2, E_3	E_0 saddle;E_1, E_2 stable node; E_3 saddle-node;
		$q_1 = g(y_1^*)$	$E_0, E_1, E_2, E_3, E_2^*$	E_0, E_2^* saddle;E_1 stable node; E_2 saddle-node; E_3 unstable node;
		$g(y_1^*) < q_1 < g(y_2^*)$	$E_0, E_1, E_2, E_3, E_2^*$	E_0, E_2^* saddle;E_3 unstable node; E_1, E_2 stable node;
	$g(y_1^*) = g(y_2^*)$	$q_1 = g(y_1^*)(g(y_2^*))$	E_0, E_1, E_2, E_3	E_0 saddle;E_1 stable node; E_2, E_3 saddle-node;

AIMS Press